Preprint
UCRL-JC-149384

Horizontal and Slant-Path Surveillance with Speckle Imaging

C.J. Carrano and J.M. Brase

This article was submitted to: 2002 AMOS (Airforce Maui Optical Station) Technical Conference, Wailea, Maui
September 15 – 21, 2002

U.S. Department of Energy

Lawrence
Livermore
National
Laboratory

September 13, 2002

HORIZONTAL AND SLANT-PATH SURVEILLANCE WITH SPECKLE IMAGING

Carmen J. Carrano and James M. Brase
Lawrence Livermore National Laboratory, 7000 East Avenue, Livermore, CA 94550

ABSTRACT

A fundamental problem in providing high-quality surveillance images recorded over long horizontal or slant paths is the blurring caused by atmospheric turbulence, which reduces both the resolution and contrast. The objective of the work reported here is to develop a capability for long-range imaging through the atmosphere that is not limited by the atmosphere but only by the fundamental diffraction limit of the optics. This paper describes our recent horizontal and slant-path imaging experiments of point targets and extended scenes as well as simulations of point targets in comparison to experiment. We show the near-diffraction limited resolution results obtained using bispectral speckle-imaging techniques. The experiments were performed with an 8-inch diameter telescope placed either in a field, on a rooftop, or on a hillside and cover ranges of interest from 100 meters up to 10 km. The scenery includes resolution targets, people, vehicles, and other structures.

Keywords: horizontal-path imaging, slant-path imaging, bispectral speckle imaging, extended scene reconstruction, atmospheric measurements

1. INTRODUCTION

For many years, atmospheric effects in astronomical[1,2] and satellite imagery[3] have been corrected by the application of bispectral speckle imaging techniques. The common aspect between these applications is that the telescope is pointing up through the atmosphere and the object being imaged typically subtends an angle smaller than the isoplanatic angle. In a recent paper[4] we investigated the performance of a bispectral speckle-imaging algorithm when the telescope images extended scenes through a horizontal or slant path through the atmosphere. We found that in many cases it is possible to obtain near diffraction-limited imaging performance using sub-field speckle processing. In this paper we will review the results obtained previously and show new results with point sources over a short horizontal path and compare them with simulated data.

2. PREVIOUS RESULTS

2.1 Equipment

Our speckle imaging system consists of the following equipment:

Telescope:	Celestron 8-inch diameter Schmidt-Cassegrain Focal length of 2032 mm, 2-inch central obscuration
Camera:	Qimaging Retiga 1300, 12-bit CCD camera, 1280 by 1024 pixels, 6.7 by 6.7 μm pixel size, Readout noise level of 8 e-, minimum exposure time 40 μs
Other Optics:	3x Barlow lens to achieve Nyquist sampling
Computer:	PC laptop with IEEE1394 connection for data acquisition and image processing

2.2 Experiments

Experiments were performed either from the rooftop of a two story building at LLNL or from a hillside 500 feet above a road looking out at various distances. Figure 1 shows the hillside telescope location along with the target locations.

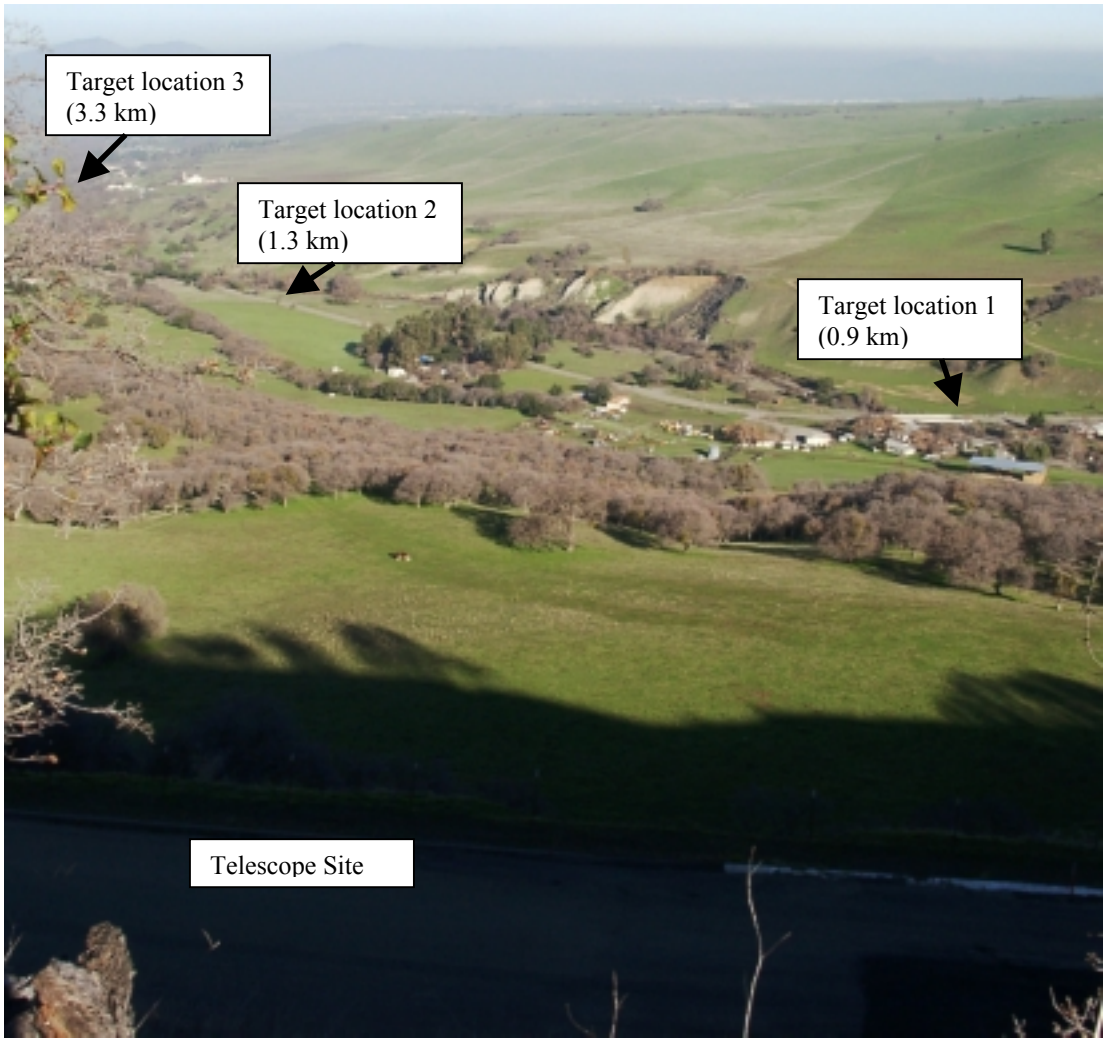

Figure 1: Digital camera picture showing hillside telescope site and the target locations. A person or people and resolution targets were placed at each of the three target locations, 0.9, 1.3, and 3.3 km distance. The telescope site is at an altitude of 500 feet (152 meters) above the target locations.

2.3 Image processing

In Ref. 4 we describe the details and rationale of the sub-field image processing using bispectral speckle-imaging techniques. The primary processing steps are summarized in Figure 2. After obtaining the raw camera images, we account for bad pixels due to any dust that may be on the camera CCD by replacing them with the average of the surrounding good pixels. The frames are then registered to each other from applying the shifts calculated from frame to frame cross-correlation. The large image data cube is next split up into sub-fields, which are overlapped by 50%. The sub-fields are then apodized and speckle processed. Finally, the processed tiles are reassembled to form the full sized image.

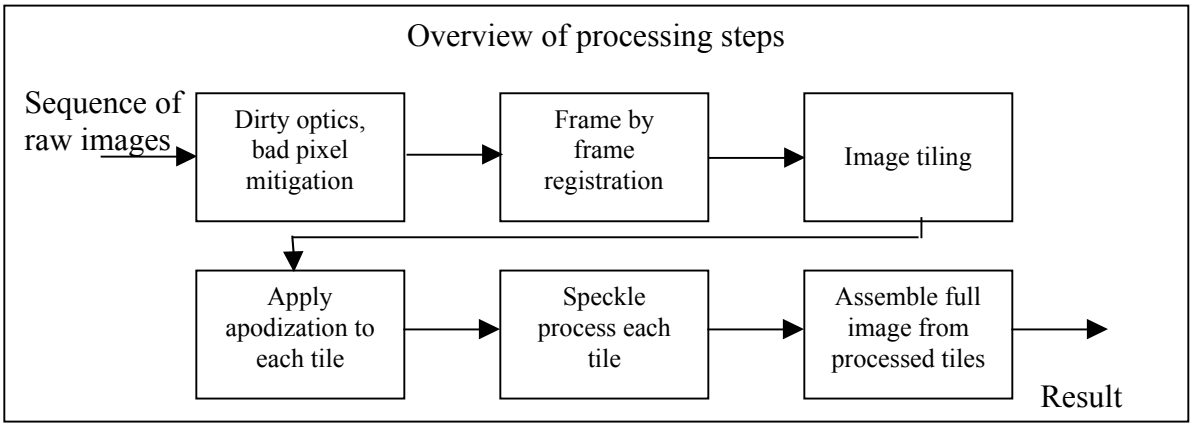

Figure 2: Block diagram overview of processing steps for producing enhanced images of extended scene, horizontal path imagery via speckle processing.

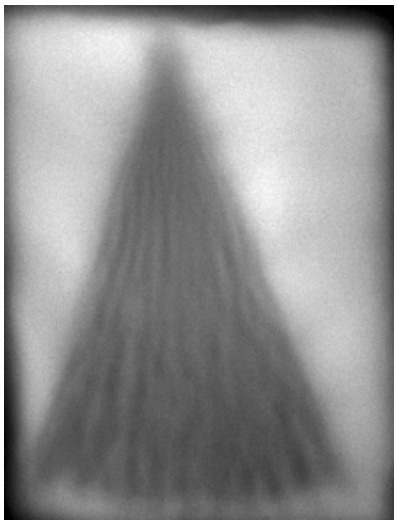

a. Example frame

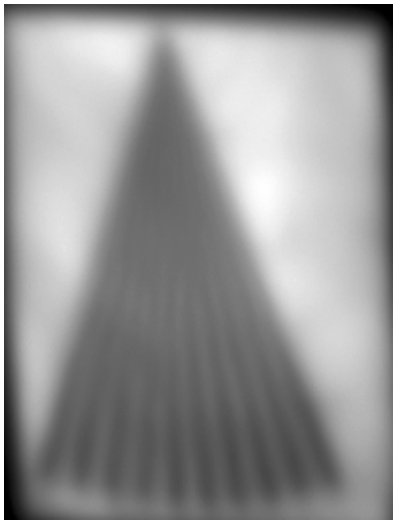

b. Shift and add (50 frames)

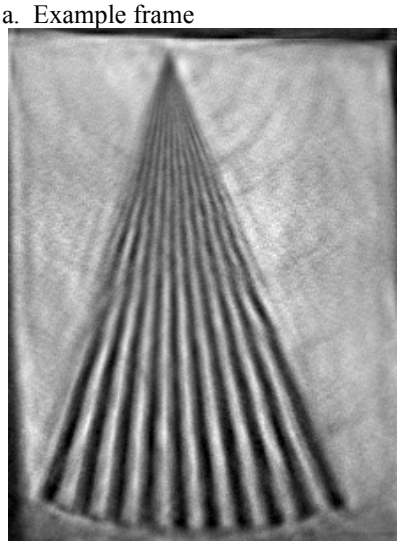

c. Speckle tile processed (512x512 sized tiles)

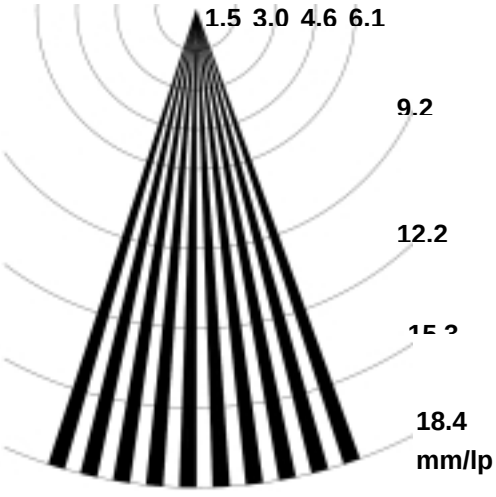

d. Ground truth for fan object

Figure 3: Results from fan target imaged at 0.5 km range with 5 ms exposure time on a hot summer day.

2.4 Results

We now show highlights of results previously obtained. The first result, displayed in Figure 3 is that of a fan target acquired at 0.5 km range from a 2-story building rooftop. We show an example frame, a shift and add result, as well as the sub-field speckle processed result. The tile size used in this case was 512x512 pixels with 60% Hanning apodization, and r_0 was set to 1.25 cm. We are able to observe modulation nearly down to the diffraction limit of 1.4 mm.

The next few results were acquired from the telescope site as shown in Figure 1. Figure 4 shows a raw frame, the shift and add result, and the speckle-tile processed result of a person standing at 0.9 km distance, target location #1 in Figure 1. The processing parameters for this case were 256x256 sized tiles, 60% Hanning window apodization, and an r_0 of 2.0 cm. After speckle-tile processing, the image of the person is sharper and crisper, and in fact the person is now recognizable. The same observation holds true for the next result shown in Figure 5, which is the same person, but standing at 1.3 km distance. He is also holding a box with the word "MAGELLAN" on it whose letters are 1.6 cm tall, and clearly readable in the speckle-tile processed image. The next result is of two people and resolution targets at 3.3 km distance and is shown is Figure 6. In the speckle-tile processed image, small details about the people are more clearly visible as are the resolution targets.

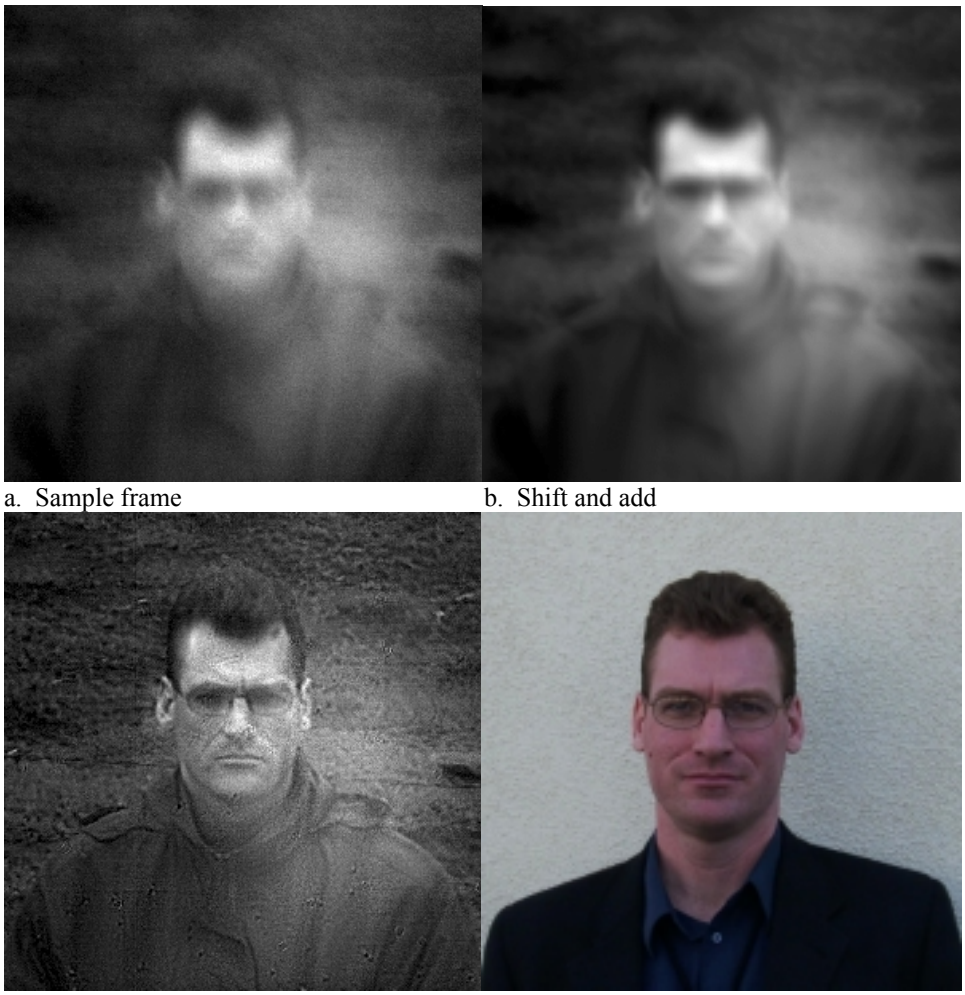

a. Sample frame b. Shift and add

c. Speckle tile processed d. Digital photograph of our subject

Figure 4: Results of a person imaged at 0.9 km distance on a cool winter morning.

a. Shift and add (100 frames)

b. Speckle tile processed (256x256 pixel sized tiles)

Figure 5. Results of person imaged at 1.3 km distance on a cool winter morning.

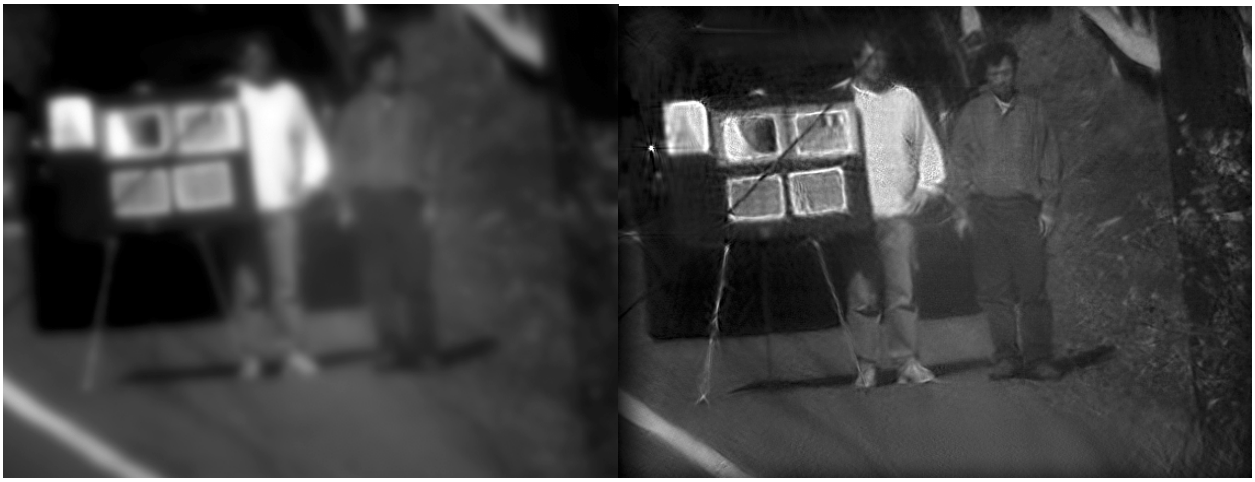

a. Shift and add (100 frames)

b. Speckle tile processed (256x256 pixel sized tiles)

Figure 6: Results of people and resolution targets imaged at 3.3 km distance on a warm breezy morning.

3.0 HORIZONTAL PATH SIMULATIONS

Since the previously reported tests, we have performed additional experiments, imaging both extended scenes and point sources. To more fully understand the results we are obtaining, we would like to model the imaging system and simulate the speckle data. In order to model the data properly, we need to know the atmospheric profile (C_n^2) over the imaging path. Because much of the data is over complicated slant paths, it is difficult to get an accurate measure of the C_n^2 profile to put into our models. To simplify the geometry and to validate our models, we decided to perform the simplest test case — imaging point sources on a horizontal path over constant terrain.

3.1 Calculating atmospheric parameters from experimental data

For our point source experiments we constructed a point source array from green LED's with variable point source spacing. A picture of the unapertured array is displayed in Figure 7. The LED's can then be apertured down to below the diffraction limit of the telescope for the range of interest. For this experiment we mounted the array on a tripod and placed it at a range of 100 meters from the telescope. Some sample frames are shown in Figure 8. When imaging at 100 meters, the field of view is quite small, which means that only the first five LED's are visible.

Figure 7: Green LED array with source spacings of :
0.5 cm, 1.0 cm, 1.5 cm, 2.0 cm, 2.5 cm, 3.0 cm, 4.0 cm , and 5.0 cm

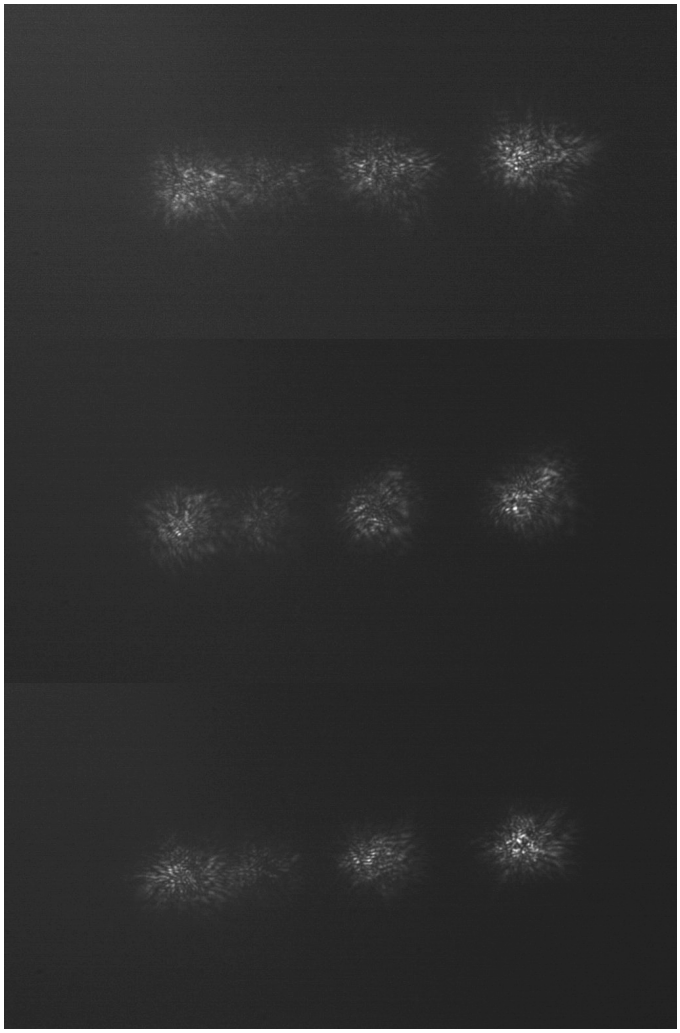

Figure 8: Three sample frames of 5 of the point sources at 100 m range, exposure time = 8 ms.

From the data it is possible to estimate the average r_0 over the path. We estimate r_0 by first extracting out an isolated point source, calculating the radial average from the centroid for each frame, and averaging all 100 radial averages together. Next, we compare this to the radial average of a model for the short exposure point spread function (PSF). The short exposure PSF is the Fourier transform of the short exposure MTF, given by [5] and [6]:

$$\tau_{short} = \tau_0(f)\exp\left[-3.44\left|\frac{\lambda f}{r_0}\right|^{5/3}\left(1-\alpha(\lambda f/D)^{1/3}\right)\right] \quad (1)$$

where $\tau_0(f)$ is the telescope's diffraction-limited optical transfer function, D is the telescope diameter, and α is a parameter that varies from 1, when phase effects are dominant(near field), to 0.5, when amplitude and phase effects have equal importance(far field)[8]. Since $D >> (L\lambda)^{1/2}$, then we can consider α to be a constant near 1[6]. As it turns out, r_0 = 6 mm and α = 0.9 gave the best match to the data. Figure 9 shows the comparison between the PSF radial averages.

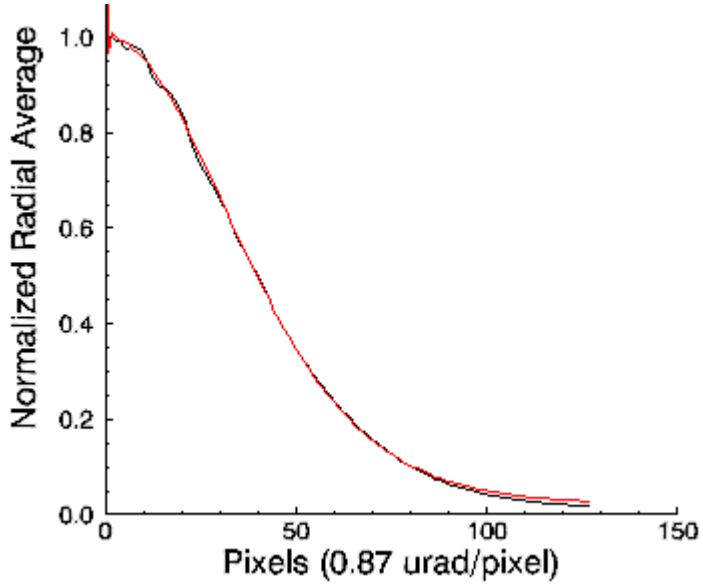

Figure 9: PSF radial average comparison between 100 meter horizontal path data (black) and model (red)with r_0 = 6 mm and α = 0.9.

From the r_0 value, and knowing that the imaging path is a true horizontal path over constant terrain, we assume Cn^2 to be constant over the path. We can solve for Cn^2 starting with the spherical wave formulation for r_0:

$$r_0 = 2.1\left[1.46k^2\int_0^L Cn^2(h)\left(\frac{L-h}{L}\right)^{5/3}dh\right]^{-3/5} \quad (2)$$

where k is the optical wave number ($2\pi/\lambda$), L is the imaging distance from telescope to the object, and h is the location of the turbulent layer. Solving for Cn^2 yields:

$$Cn^2 = \frac{0.16 r_0^{-5/3}\lambda^2}{L} \quad . \quad (3)$$

Plugging in the numbers, r_0 = 6 mm, λ = 530 nm, and L = 100 m, we obtain Cn^2 = 2.26e-12.

Another useful parameter to calculate over the path is the isoplanatic angle, θ_0, which is the angle over which the PSF stays relatively constant, or for which the variance of the relative phase between two rays is 1 rad^2. It is also an integral over Cn^2 and the path[7]:

$$\theta_0 \equiv \left[2.914 k^2 (\sec z)^{8/3} \int_0^L dh C n^2(h) h^{5/3} \right]^{-3/5} \tag{4}$$

Holding Cn^2 constant, setting "sec z = 1" for a constant Cn^2, and performing the integral, we obtain,

$$\theta_0 = \left(1.093 k^2 C n^2 L^{8/3} \right)^{-3/5} \tag{5}$$

Plugging in our numbers, we calculate a θ_0 of 18 μrad. This means that at a source distance of 18 urad * 100 meters, or 1.9 mm, the speckle patterns should begin to decorrelate. This is consistent with the data, as none of the speckle patterns appear to have much correlation between them in a qualitative sense. (Note: The topic of comparing isoplanatic angle calculations from cross-correlation versus the above equations will be the subject of work in the coming months.)

3.2 Distributed turbulence simulations

We have developed a capability to simulate speckle imagery with distributed turbulence. We model the distributed turbulence by splitting the path into atmospheric layers of a certain depth. At the center of each layer we insert a properly sampled Kolmogorov phase screen with a given r_0 value. Using Fresnel propagation, we propagate each point source from its origin through each phase screen to the aperture. Once the complex field reaches the aperture, we apply the aperture function, and fresnel propagate through free space, back to the camera. Figure 10 illustrates the concept.

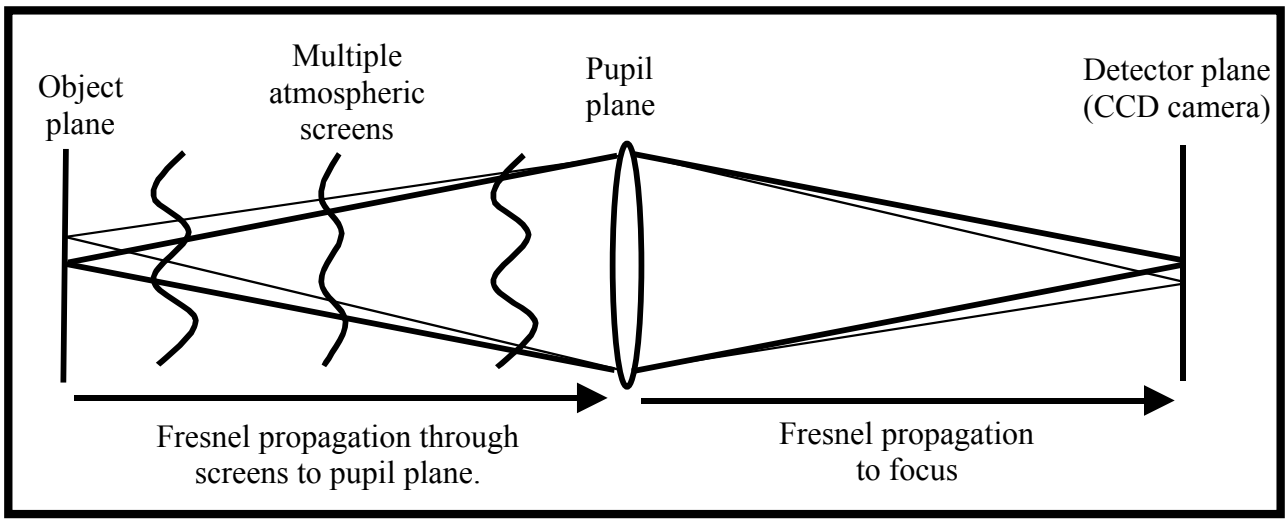

Figure 10: Illustration of distributed turbulence simulation

To simulate the experimental data we chose to use five atmospheric screens spaced 20 meters apart over the 100-meter path. From Cn^2, we can calculate the needed r_0's for each screen. As it turns out, we obtained the best match to the data when the r_0's were set to 1.3 cm, which is only slightly less than the calculated value of 1.5 cm. See Figure 11 for a comparison of sample frames of the simulated data compared to the experimental data, and Figure 12 for a radial average comparison. The data resemble each other in terms of the spot size and numbers of speckles. What is not captured in the simulation is the effect of either the finite exposure time or the finite bandwidth of the LED sources (~30 nm), which causes radial spreading of the speckles as they get further from the center.

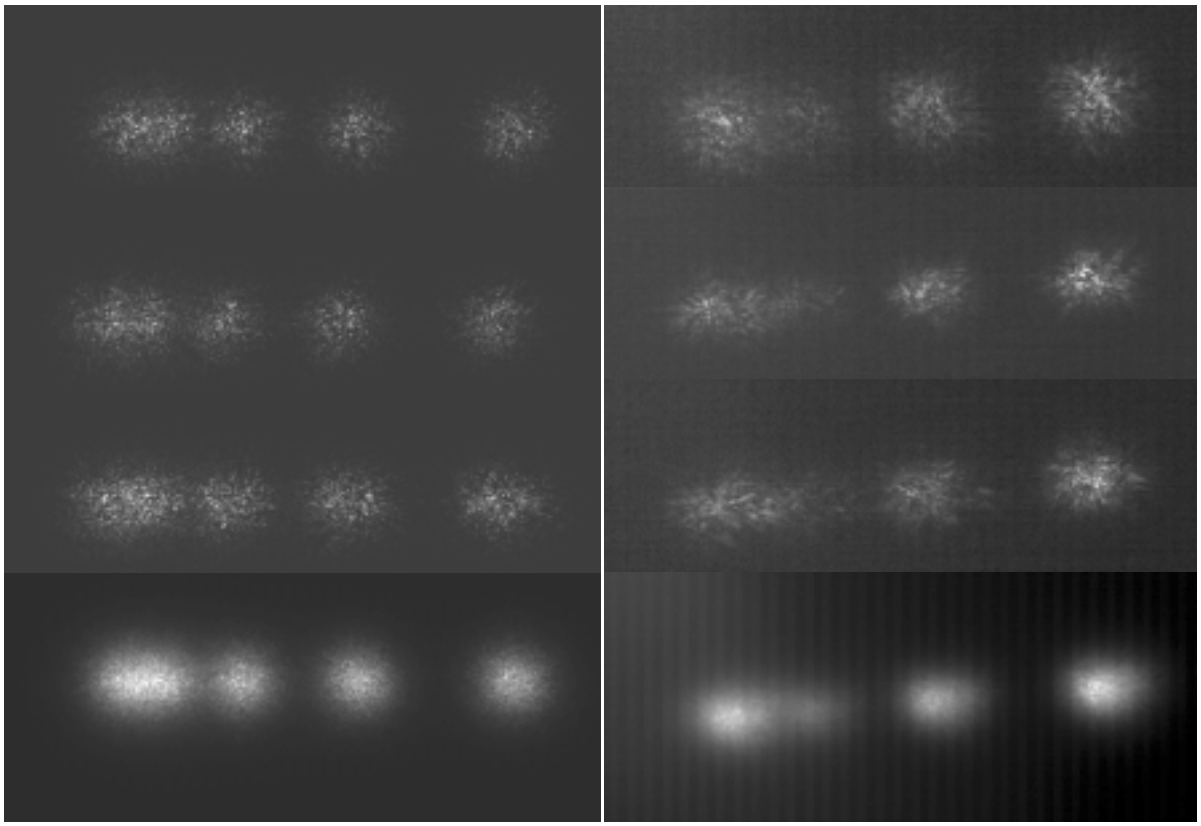

Figure 11: Left: Sample frames from multi-point source distributed turbulence simulations, with the bottom frame showing the shift and add result with 30 frames. Right: Sample frames from experimental data with the bottom frame showing the shift and add result with 100 frames.

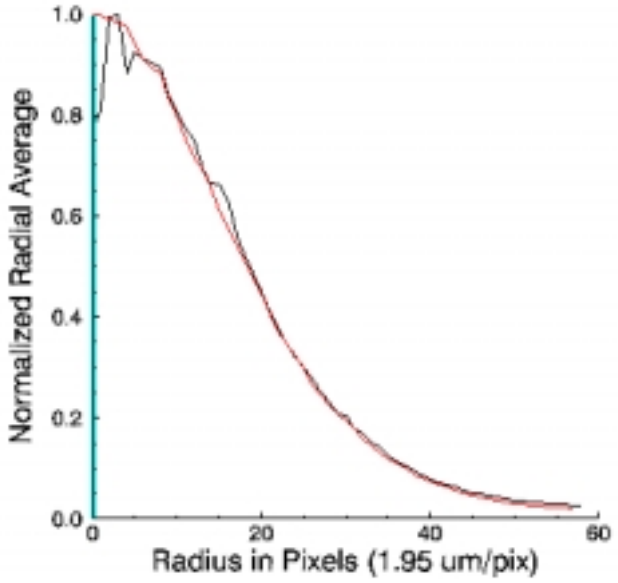

Figure 12: PSF radial average comparison between 100-meter horizontal path data (red) and simulated data (black)

4.0 CONCLUSIONS

We have demonstrated a long-range horizontal/slant path video surveillance system using speckle-imaging techniques. It is possible to obtain near diffraction-limited results in many cases and much improved resolution in others. This surveillance technology could be fielded from a number of platforms (eg. hillside, tower, UAV) for a number of surveillance purposes (eg. personnel and vehicle identification.) In an effort to better understand the mechanisms at work and to help optimize our processing parameters, we are developing a simulation capability, which needs to be validated with experimental data. By successful comparison and matching of point source data, both experimental and simulated, we have taken a first step along the road to validating the simulations.

ACKNOWLEDGEMENTS

We would like to acknowledge the help of Kevin Baker, Doug Poland, Scott Wilks, Karen Hanzi, and Peter Young for helping to perform the experiments, and Jack Tucker for building the LED array.
We would also like to thank Scot Olivier, Kevin Baker, and Kai LaFortune for being willing imaging subjects.
Work performed under the auspices of the U.S. Department of Energy by the Lawrence Livermore National Laboratory under contract No. W-7405-ENG-48.

REFERENCES

1. A. W. Lohmann, G. Weigelt, and B. Wirnitzer, "Speckle masking in astronomy: triple correlation theory and applications," Appl. Opt. **22**, 4028-4037 (1983)
2. H. Bartelt, A. W. Lohmann, and B. Wirnitzer, "Phase and amplitude recovery from bispectra," Appl. Opt. **23**, 3121-3129 (1984)
3. T. W. Lawrence, D. M. Goodman, E. M. Johansson, and J.P. Fitch, "Speckle imaging of satellites at the U.S. Air Force Maui Optical Station", Appl. Opt. **31**, 6307-6321 (1992)
4. C. J. Carrano, "Speckle Imaging over Horizontal Paths", Proceedings of the SPIE -High Resolution Wavefront Control: Methods, Devices, and Applications IV, **4825** (2002)
5. D. L. Fried, J. Opt. Soc. Am. **56** 1372-9 (1996)
6. J. W. Goodman, *Statistical Optics*, New York: Wiley (1985)
7. A. Quirrenbach, "Observing Through the Turbulent Atmosphere", Chapter 5 Course Notes, UCSD
8. H. Beaumont, et. al., "Image qualite and seeing measurements for long horizontal overwater propagation", Pure Appl. Opt. **6**, 15-30 (1997)

This work was performed under the auspices of the U.S. Department of Energy by the University of California, Lawrence Livermore National Laboratory under contract No. W-7405-Eng-48.